

Using a Drone Formation with Sectored Antennas in Search-And-Rescue: Heuristics for Orienting Drones and Moving the Formation

Samuel Pell, Andreas Willig

*Department of Computer Science and Software Engineering, University of Canterbury, Christchurch, New Zealand
{sam.pell, andreas.willig}@canterbury.ac.nz

Abstract—Recently there has been interest in using drones/unmanned aerial vehicles in search-and-rescue applications. Here we apply a formation of drones equipped with sectorised antennae to navigate to a transmitter using Direction of Arrival (DoA) estimation to navigate. We present results indicating that the error of the DoA estimate is dependent on the DoA and evaluate a mitigation technique, finding that incrementally changing the drone orientation across the formation reduces the DoA estimation error. Further, we investigate a “dumbbell” formation in which the two “weights” generate independent DoA estimates, the difference between which are used to broadly classify the distance to the transmitter. We found that the choice of distance thresholds and relative direction of the transmitter substantially changes the performance of this distance heuristic.

Index Terms—direction-of-arrival estimation, search and rescue, UAV, UAV formations

I. INTRODUCTION

Unmanned Aerial Vehicles (UAV) or drones have recently attracted a lot of interest in search-and-rescue (SAR) applications [1]–[5], as they can potentially cover large search areas quickly. Different sensor modalities can be used to first make a detection of a lost person and then narrow down its location sufficiently to guide a rescue team to the right place. In [6] we have assumed that a missing person is equipped with a wireless transmitter (e.g. a smartphone) which transmits wireless signals regularly, and we considered what path an individual drone should follow in an unknown environment *before* it detects a wireless signal for the first time, with the goal of making that first detection as early as possible. Depending on transmit power and channel properties, the distance between drone and transmitter at the time of first detection can still be too large to send out a rescue team, and we need to narrow down the location of the transmitter further.

We seek to extend our previous work [6] and consider the question of how we can localise a wireless transmitter to a given accuracy (in the order of a few tens of meters) and in the shortest possible time after the first detection. Instead of using just a single drone we propose to use a rigid formation of drones, each equipped with a sectored antenna, to repeatedly obtain estimates of the bearing between the drone formation and the transmitter, and use these estimates to reduce the distance to the transmitter quickly until the formation is sufficiently close.

This approach raises a number of design questions concerning “static” properties of the formation, e.g. its shape (line or circle or ball or ...), the configuration of individual drones (in particular the number and characteristics of antenna sectors), the orientation of individual drones within the formation, and the methods used for bearing estimation. In this paper we investigate these questions through simulations, considering different options for these characteristics. Furthermore, we investigate the “dynamic” question of where the drone formation should move next (path planning), given one or more observations of a wireless signal and resulting bearing estimates. In particular, we propose a formation shape (the “dumbbell”) which allows to generate two bearing estimates in parallel from different parts of the formation, and derive from these a coarse classification of whether the transmitter is “near” or “far”. Based on this classification we then decide the “stepsize”, i.e. by how much we move in the overall direction derived from the two available bearings, before deciding again. In particular, in this paper, we make the following contributions:

- We present simulation results giving some insight into the trade-offs between the number of sectors or antenna directivity on the one hand and RMSE for a bearing estimate on the other hand. Similarly, we present results for the RMSE versus the orientation of drones, and we consider selected formation shapes.
- We consider a particular formation shape, the “dumbbell”, which can be imagined as two “independent” formations at some distance, but linked together. In this formation the two “weights” at the end points generate independent bearing estimates, which then are combined towards an overall bearing estimate, and which we furthermore use to perform a coarse classification of the distance between transmitter and formation into one of a very small number of regions. The stepsize for the formation is chosen based on that classification result. We show results indicating that the choice of regions and stepsizes does significantly impact the time for the formation to get within ten meters of the transmitter.

The remaining paper is structured as follows: after commenting on related work in Section II, we introduce in Section III our system model, the DoA estimation and DoA estimate fusion techniques used throughout the paper. Section IV

then describes our simulator validation, explores the effect of DoA on the DoA estimate error plus a possible mitigation technique, and then develops and tests a heuristic for categorising the distance to the transmitter, allowing the formation to choose its step size when navigating to the transmitter. Finally, Section V summarises our results and novel contributions and outlines possible future research directions.

II. RELATED WORK

In the literature, several works have explored using drones and DoA estimation techniques to localise a transmitter [7]–[11]. Most focus on a single drone [7]–[10] or require communicating sample-level data between the swarm UAVs [11].

References [7], [8] both use a single antenna DoA estimation scheme, where the drone physically rotates, measuring the direction in which the transmitter’s signal is strongest. They then move a set distance in the transmitter’s estimated direction. Since these schemes rely on the drones to rotate whilst stationary it not only increases the time to localise the transmitter, it also requires more energy, reducing the maximum possible flight time and range for the drone. The authors of [9] adopt a similar, single step size system, however they switch between four antennas, placed at 90° to each other to estimate the transmitter’s direction. This removes the rotation requirement, reducing the total energy usage of the DoA estimation scheme, but increases the payload.

References [10] and [11] both use a non-signal-strength based approach to DoA estimation. Reference [10] uses a single drone to repeatedly sample a periodic, repetitive signal (e.g. the short preamble signal in IEEE 802.11 packets), time-aligning them to extract phase differences and calculate the DoA. [11] relies on having multiple different swarming drones sampling the signal and using the MUSIC (multiple signal classification) algorithm to estimate the transmitter bearing. However, this requires each drone to communicate its raw samples to a centralised computation node, which is bandwidth inefficient and limits the number of drones possible in any swarm. Neither [10] or [11] address navigating to the transmitter, purely determining the DoA of its signal.

III. SYSTEM MODEL

To simulate the SAR scenario laid out in Section I, we assume the lost person has a short range transmitter which continuously transmits an unspecified distress signal. The searchers deploy K drones, each equipped with an antenna consisting of M equal-sized sectors, to locate and travel to the transmitter’s location. The following sections outline how an individual drone estimates the transmitter location and how the formation combines their individual estimates together.

We assume that the target is static, and that the search area does not have any obstacles limiting signal propagation or the free movements of drones. All channels are assumed to be line-of-sight channels which we characterise only through their SNR, ignoring the details of detection. There is no interference, and we furthermore assume that the communication between drones is done over perfect channels not

overlapping with the channel used by the target, i.e. we ignore any delays or packet losses between drones in the course of signal combining. There is also no shadowing between drones. The decision about where the formation will go next is carried out by one particular drone, the “lead drone”. We treat the drones themselves as simple points and do not use a precise dynamic model for them. We assume that drones move at an average speed of 5 m/s. We finally assume that all drones share a pre-arranged coordinate system, so that all bearings are using the same reference.

A. Direction of Arrival (DoA) Estimation on Single Drones

We denote the continuous transmission signal from the target by $s(t)$ and its sampled version as $s(n)$ with $n \in \mathbb{N}_0$. Each drone k in the formation samples the continuous transmission $s(t)$ using each of the M sectors of its antenna. As drone k samples $s(t)$ incoherently and below the Nyquist rate of the signal,¹ we consider $s(n)$ to be complex-valued random noise with zero mean and variance γ_k :

$$s(n) \sim \mathcal{CN}(0, \gamma_k). \quad (1)$$

The received signal at drone k , sampled using sector m , is

$$r_{k,m}(n) = \xi_m(\phi_k) s(n) + N_0(n), \quad (2)$$

where $\xi_m(\phi_k)$ is the attenuation of the m -th sector of the antenna at the DoA ϕ_k and $N_0(n)$ is complex additive noise introduced by the receiver front-end and environmental interference. The received signal power of N measured samples of the signal from sector m at drone k is

$$\epsilon_{k,m} = \frac{1}{N} \sum_{n=0}^{N-1} |r_{k,m}(n)|. \quad (3)$$

To model the radiation pattern of each antenna sector, the Gaussian-like shape from [12] is used. In [12], the beam pattern of sector m of the antenna is approximated as

$$\xi_m(\phi) = \alpha_m e^{-\left(\frac{\mathcal{M}(\phi - v_m)}{\beta_m}\right)^2}, \quad (4)$$

where v_m is the direction of sector m ’s maximum gain (α_m), β_m is the beamwidth of the main beam, and

$$\mathcal{M}(\phi) = \text{mod } 2\pi(\phi + \pi) - \pi. \quad (5)$$

This model is based on the observations made in [13], [14] that most directional beam patterns have an approximately Gaussian-like shape. For the special case of Equal Sector Antennas (ESA) where each sector has the same beamwidth and gain, and each sector covers $\frac{360^\circ}{M}$, the beamwidth can be parameterised using the side sector suppression a_s , where

$$\beta = \frac{2\pi}{M\sqrt{-\ln(a_s)}}. \quad (6)$$

This special case is applicable when the sectored antenna is assembled from M sub-antennas of the same make and model,

¹This is natural as we do not make any assumption about the transmitted signal, in particular we do not try to de-modulate. Furthermore, complexity reasons suggest to limit the sampling bandwidth.

which the receiver can electronically switch between. In this paper we assume all drones are equipped with ESA antennas.

To estimate the DoA of the transmitted signal, each drone k uses the Three-Stage Simplified Least Squares (TSLs) method described in [12]. This method has three stages:

- 1) **Sector selection:** select the L sectors surrounding the sector-pair (a sector pair refers to two neighbored sectors) with the strongest received signal as \mathcal{L}_k .
- 2) **Sector-Pair DoA Estimation:** Calculate the noise-centred powers for each sector i in \mathcal{L}_k as $p_{k,i}$,

$$p_{k,i} = \epsilon_{k,i} - \sigma_w, \quad (7)$$

where σ_w is the measured noise power on the channel.² Discard any sectors with negative noise-centred powers. For each remaining possible sector pair $i, j \in \mathcal{L}_k, i \neq j$, calculate the estimated DoA as

$$\hat{\phi}_{k,ij} = \bar{v}_{k,ij} + \frac{\beta^2}{4(v_i - v_j)} \left(\ln \frac{p_{k,i}}{p_{k,j}} - 2 \ln \frac{\alpha_i}{\alpha_j} \right), \quad (8)$$

where $\bar{v}_{k,ij} = \frac{v_i + v_j}{2}$. Note that (8) only holds for sectors with identical beamwidths. If all sectors are eliminated due to negative noise-centred powers, we use the maximum energy DoA estimation method outlined in [15] to estimate the DoA.

- 3) **DoA Fusion:** All of the different DoA estimates, $\hat{\phi}_{k,ij}$ are combined into a final DoA estimate for each drone $\hat{\phi}_k$ as

$$\hat{\phi}_k = \arctan \left(\frac{\sum w_{k,ij} \sin \hat{\phi}_{k,ij}}{\sum w_{k,ij} \cos \hat{\phi}_{k,ij}} \right), \quad (9)$$

where $w_{k,ij} = p_{k,i} p_{k,j}$.

An analysis of TSLs's complexity is provided in [12].

B. Combining DoA Estimates

To combine the different estimates of the transmitter's DoA, each member of the formation sends its data to the lead drone. The lead drone combines these results using the method of combining circular random variables proposed in [16]:

$$\hat{\phi} = \arctan \left(\frac{\sum \sin \hat{\phi}_k}{\sum \cos \hat{\phi}_k} \right). \quad (10)$$

This is an unweighted version of the method used in Step 3 of the TSLs method discussed above and has a complexity of $\mathcal{O}(K)$. This assumes the estimated per-drone DoA values will all be similar for all drones in our formation, i.e. that the target is far away compared to the maximum separation between the drones. The effects of distance to the difference in the angle estimated by two or more drones will be discussed more in Section IV-B.

It is to be noted that in our paper we only generate a bearing estimate via Equation (10) and do not attempt to actually localise a transmitter (by calculating an estimate of its coordinates, e.g. using the Stansfield algorithm [17]). This is

²We assume that each drone measures its receive noise power before start of flight, while the drone is still at a large distance from the transmitter.

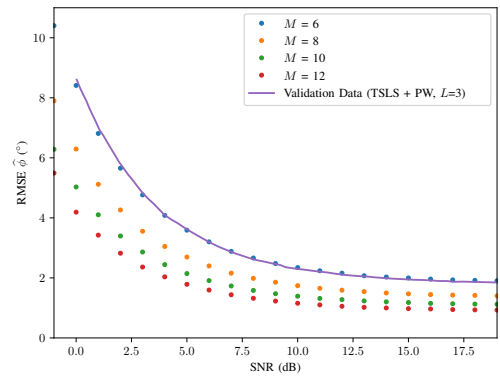


Fig. 1: As the number of sectors (M) increases, the root-mean-squared-error (RMSE) of bearing estimates ($\hat{\phi}$) decreases for all simulated signal-to-noise-ratios (SNR). The validation data is taken from Figure 6 of [12], where $M = 6$ and $a_s = 0.4$.

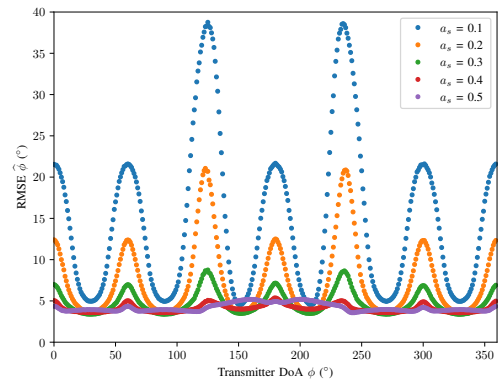


Fig. 2: The RMSE of the estimated DoA is dependent on both the DoA and the antenna's directionality (measured by a_s). $M = 6$.

because after the very first detection of the transmitter signal the formation may still be very far away from the transmitter and the bearings estimated by the individual drones can be quite similar, introducing a large average error in a distance estimate. Instead of trying to estimate the distance, we only attempt to classify it coarsely into one of a small number of regions and decide a stepsize for the formation based on that.

Since drones can only carry a limited number of sectors for weight and space reasons, they are also limited in the accuracy they can achieve. To illustrate this, in Figure 1 we show the root mean-square error (RMSE) of the bearing estimate for varying SNR of the received signal and for varying number of sectors, assuming $a_s = 0.4$ (see below). In Figure 2 we show the RMSE for $M = 6$, varying side-sector suppression a_s and varying transmitter bearing. The results indicate that more directional antennas (smaller a_s) have a higher RMSE, presumably due to the reduced overlap between sectors, leading to increased error in the DoA estimate when one sector is pointed towards the transmitter (as there is less information on the location).

IV. SIMULATIONS AND RESULTS

We now discuss simulation results exploring the system described in Section III. The simulator was implemented in Python.³ We look at two major factors which impact the overall SAR application: minimising DoA estimate error by changing the orientation of drones in the formation and analysing a possible heuristic to determine how far the formation should move towards the transmitter after an updated bearing estimate and distance classification has been computed.

Except where mentioned all simulations have been run for 100 000 replications. Error bars are included only when the 95% confidence intervals are significant enough to be seen. Similarly, unless mentioned otherwise, every drone in these simulations has an $M = 6$, $a_s = 0.4$, ESA antenna (taken from [12]) and the TSLS method takes $N = 100$ samples of the signal and selects $L = 3$ sectors in stage 1.

We validated our simulator by comparing it to the results presented in [12]. The validation data was extracted from the paper and overlaid on Figure 1. Since the RMSE values from our simulator closely match those presented in [12] we consider our simulator validated.

A. Effect of Drone Orientation on the Estimated DoA

As we have highlighted in Figure 2, the error in the DoA estimate is dependent on the DoA. To partially mitigate this effect, we combine the estimates from all drones. Furthermore, we hypothesise that the orientation of each drone in the formation will also change the overall RMSE. As such, we compare the RMSE of four drone orientation schemes:

- **Uniform:** All drones have the same orientation. We have considered the default orientation as always pointing towards “true-north”.
- **Incremented:** Each of the K drones in a formation has a different orientation, with drone k with a M -sectored antenna having an orientation of $\frac{360k}{MK}^\circ$ from the “true-north” bearing.
- **Partitioned:** The formation is broken into G partitions. Each partition has a different orientation, with partition g having an orientation of $\frac{360g}{G}^\circ$. All drones within one partition have the same orientation.
- **Random:** Each drone has a random orientation.

To compare these four options, we simulate a nine-drone array in two different formations as the SNR changes. The drones are organised into two formations: one where all the drones are in a single line, orthogonal to the transmitter, and another for a circle of drones (Figure 3). The transmitter and drone formation centre are placed randomly on a 10 km by 10 km field. In the line formation each drone is placed 10 m apart and the circle formation has a radius of 20 m. For each SNR, formation, and orientation option, we performed 10 000 replications, and the RMSE results including error-bars are shown in Figure 4.

Figure 4 shows that, as expected, the relative orientation of each member significantly affects the RMSE of the formation’s

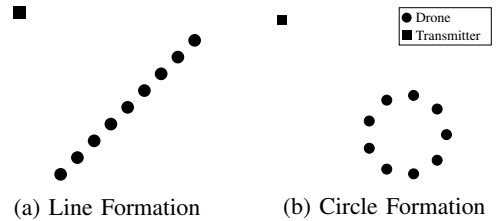


Fig. 3: The two formations simulated.

DoA estimate. At high SNR values (≥ 6 dB), these results do not reveal differences between the non-uniform orientation options, which all perform better than the Uniform orientation option. For lower SNR values (< 6 dB), the Partition and Uniform orientations perform indistinguishably, and both perform worse than the Incremented and Random options. As the SNR decreases, the Incremented orientation scheme begins to perform better than the Random scheme.

It is worth noting that the overall formation structure (line vs circle) does not appear to have much influence on the RMSE. However, we need to keep in mind that we have used a somewhat simplified system model without any signal shadowing by drones. We do expect that a more realistic modelling of shadowing can have an impact on the results, this is a worthwhile topic for future work.

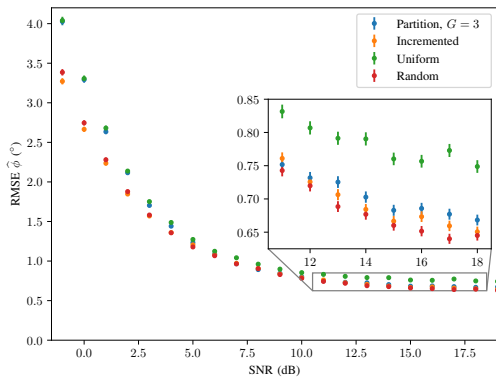
B. Dumbbell Formation and Variable Stepsize Scheme

Our ultimate goal is to use bearing estimates to get within a set range of the transmitter in as short a time as possible. To enable comparison with relevant schemes from the literature, we adopt the behaviour used in [9] and [7], in which the searching drone(s) alternate between periods of movement and signal measurement periods. This was necessary since in Reference [7] the drones could only sample one spatial direction and had to physically rotate the drones to cover all sectors. This takes time and needs to be carried out in the same location for consistency. The authors of [9] also have adopted such an alternating scheme. Once a bearing estimate has been calculated, the schemes in [9] and [7] move a set distance into that direction (fixed step size). In this paper, we investigate a scheme in which the choice of step size is based on a coarse classification of the distance to the transmitter into one of a small number of regions, i.e. we adopt a variable step size. In theory, nothing in our setup speaks against performing signal measurements and choosing step sizes continuously.

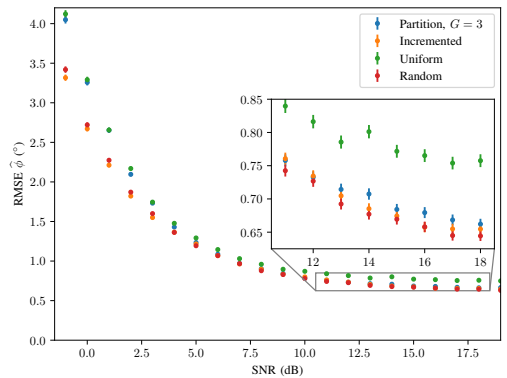
To classify the distance to the transmitter (R), we change the organisation of the drone formation to a dumbbell shape, subdividing the drones into two different circle formations (the “weights”) and arranging them as in Figure 5. Within each weight, the drone orientations are chosen according to the Incremented scheme. As a result, we can obtain two different DoA estimates (one per weight), $D = d + 2r$ metres apart, which we refer to as $\hat{\phi}_A$ and $\hat{\phi}_B$. Our object of interest now is the absolute difference in angle estimates

$$\widehat{\Delta A} = \left| \hat{\phi}_A - \hat{\phi}_B \right|. \quad (11)$$

³Available: <https://github.com/STPell/DroneFormationDOAEstimation>



(a) Line Formation



(b) Circle Formation

Fig. 4: The effect of the drone orientation schemes on the formation's DoA estimate.

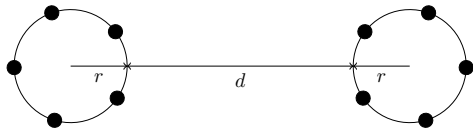


Fig. 5: The dumbbell formation.

In Figure 6 we assume that we know the bearings ϕ_A and ϕ_B perfectly and that we can calculate the correct absolute difference in angle estimate ΔA . We show how ΔA varies for given $D = 40$ m and changing bearing, assuming that the transmitter is at a known distance from the mid-point of the dumbbell. These results were generated analytically.

For the purpose of classification, we give ourselves a number of comparison distances $\{R_1, R_2, \dots, R_p\}$. Given the two estimated bearings $\hat{\phi}_A$ and $\hat{\phi}_B$, we calculate the resulting $\widehat{\Delta A}$ and also the estimated bearing $\hat{\phi}$ according to the fusion method described in Section III-B. Then, using the equivalent of Figure 6 for the given comparison distances $\{R_1, \dots, R_p\}$, we pick the comparison distance which has the largest ΔA value not exceeding $\widehat{\Delta A}$ for the (estimated) target bearing $\hat{\phi}$.

Before proceeding, we make two further observations from Figure 6. First, as the bearings approach 90° and 270° the difference in angles approaches 0 for all distances. This is as for bearings of 90° and 270° the transmitter is collinear with the formation and thus there is no difference in bearing. Secondly, in the far field ($R \gg D$), the bearing estimates of both weights are quite similar, which we illustrate in Figure 7.

To test this method, we setup a simulation to measure the classification heuristic's failure rate. A false positive is when the system categorises the transmitter as being closer than the threshold distance, when in reality it is further away than the threshold distance. A false negative is where the system categorises the transmitter as being further away than the threshold distance but in reality, it is closer. The false positive and false negative rates were simulated in two different simulation settings: one where the target is always within the threshold distance, the other where the target is

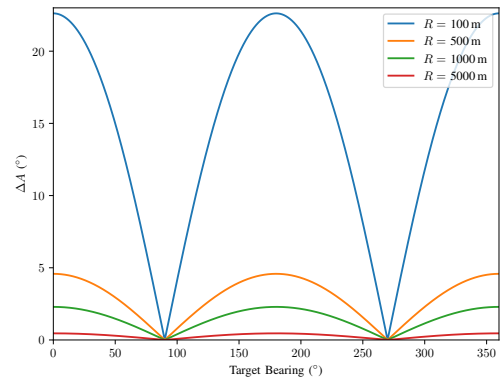


Fig. 6: ΔA varies with the direction and distance to the target. $D = 40$ m.

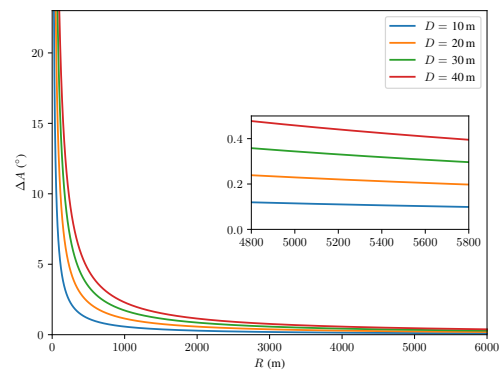


Fig. 7: How the ΔA changes with the target range (R).

placed randomly in a 10 km by 10 km field and its location is regenerated if it is closer than the threshold distance. This ensured an equal number of positive and negative replications.

All replications were run for $r = 10$ m, $D = 40$ m, with 5 drones per formation at the end of the dumbbell. The results of these simulations are shown in Figure 8. For low SNR values (< 7 dB), the thresholding heuristic is worse than tossing a fair coin at categorising the target range for the 500 m and

1 km thresholds. This is unsurprising as the ΔA threshold is small enough that it is likely below the error floor at these SNR. Interestingly, the false negative rate does not appear to be as strongly affected by the SNR. This is possibly due to the angle estimation accuracy required to categorise the far-away cases being a lot higher than the accuracy possible with this DoA estimation method even at high SNR and averaging across drones. We note that our thresholding heuristic performs much better for smaller distance thresholds, which will guide our choice for the distance thresholds $\{R_1, \dots, R_p\}$.

Based on a selection $\{R_1, \dots, R_p\}$ of distance thresholds, the resulting adaptive stepsize procedure is simply obtained by picking the step sizes to be the same as the distance thresholds, i.e. if our heuristic selects distance threshold R_i , we move R_i meters into the direction of the estimated bearing before stopping there and taking the next set of measurements.

We now present results comparing the time required to get within 10 m of the transmitter for different choices of the set of distance thresholds in our adaptive stepsize procedure, and compare these also against the fixed stepsize procedures proposed in [7] and [9]. In these simulations we assume that a measurement period takes ten seconds (during which the drones remain stationary). The target was always placed at the origin and the dumbbell formation was placed on a random bearing at a fixed distance from the transmitter. Two starting distances were manually selected (1628 m and 3628 m), ensuring different step sizes would be used through the procedure. The other formation parameters were the same as above. The received signal strength at each drone is calculated as:

$$\gamma_k = P_{\text{tx}} G_{\text{tx}} G_{\text{PL}}(d), \quad (12)$$

where P_{tx} is the transmit power (10 dBm), G_{tx} is the transmitter antenna gain (0 dB), and $G_{\text{PL}}(d)$ is the path loss at distance d . We used the free-space path loss calculated as [18]:

$$G_{\text{PL}}(d) = \left(\frac{4\pi d}{\lambda} \right)^{-2} \quad (13)$$

where d is the distance to the transmitter in metres and λ is the wavelength of the transmitted signal in metres. The transmit frequency was set to 2.45 GHz. To determine the noise power we assume a noise-floor of -174 dB/Hz across the sampling bandwidth of 2.5 MHz and a receiver noise figure of 8 dB. For comparison to [7], [9], we use a step size of 10 m. This was chosen as it is the same as the detection radius, ensuring that we do reach the stopping condition.

In Figure 9 we compare the Empirical Cumulative Distribution Function (ECDF) of the time taken to reach the target for several different threshold distance sets. We refer to each such set by its maximum step size (MSS). The blocky shape of the ECDF is caused by the extra 10 s added by each additional DoA estimation measurement, rather than the number of replications performed (100 000). For $R = 1628$ m (Figure 9a), the 200 m and 500 m maximum step size (MSS) options perform similarly, with the 200 m being slightly better in almost all cases. The 1 km options shows the worst behaviour, as it lags all other options significantly after slightly more than 500 s.

The 100 m option only starts to rise at around 500 s (i.e. much later than the 200 m and 500 m options) but closes in quickly. The main conclusion is that the choice of the distance set makes a substantial difference, and that “medium” step sizes between 200 m and 500 m should be included.

For the $R = 3628$ m case (Figure 9b), the 500 m MSS performs the best in most replications, however, the 200 m MSS case has slightly better tail-end performance. For $\approx 40\%$ of the replications, the 1 km MSS performs much better than all other options, however its performance drops compared to all other cases for the remainder. Unsurprisingly the 100 m case performs worse than all MSS options in $\approx 80\%$ of replications, however it has similar performance to the 500 m and 200 m MSS cases in the tail-end. The increase in time to the target for large MSS may be caused by two failure cases:

- Error in the DoA estimate leading to the formation moving further away from the target compared to two smaller steps with an intermediate DoA estimate.
- Over-estimating distance to target and back-tracking.

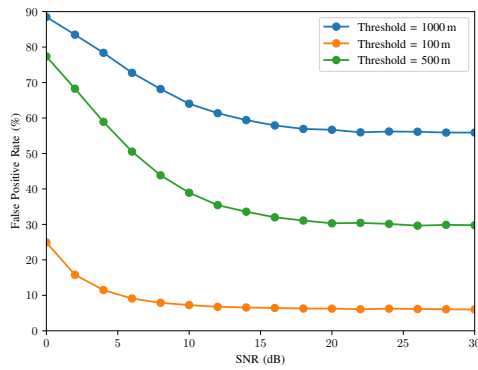
For both initial distances and all MSS choices, the variable step size method arrived at the target faster than the fixed step size method in almost all cases ($>99\%$). For $R = 1628$ m, even the poorly performing 1 km MSS option is over 800 s faster than the fixed step size case in 95% of replications. This shows that when the target is initially far away, the ability to select larger step sizes can greatly reduce the time to reach the target, even for poor MSS choices.

V. CONCLUSIONS

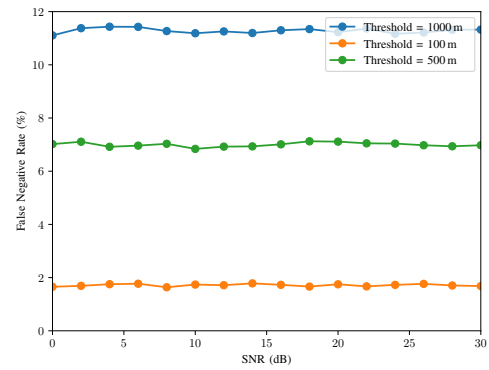
In this paper we extended our prior work [6], focusing on the stage after first detecting the transmitter, trying to localise it to an acceptable level. We use a formation of drones equipped with sectored antennas, navigating to the transmitter using DoA estimation. We found that the DoA estimate error varied with the transmitter bearing and that choosing the formation’s drone’s orientations carefully decreases the overall RMSE of the formations DoA estimate. In particular, the Incremental orientation scheme resulted in the lowest RMSE.

To reduce the total time to reach the transmitter we explored adaptive step sizes when choosing the travel distance between DoA estimate measurements. For this we used the difference in DoA estimates between two ends of a “dumbbell” formation, and coarsely classifying the distance to the transmitter. We found that this distance heuristic has promise, however the choice of thresholds and the relative bearing of the transmitter to the formation has substantial impact on performance.

There are several possible avenues for future work, the most obvious are to improve the thresholding heuristic and evolve the step size selection scheme to use continuous measurements without stationary periods. A possible improvement to the distance heuristic is to adapt the formation shape and pose based on the estimated target distance/bearing. Another question not addressed in this paper are criteria for the drone formation to decide when it has reached the transmitter. A further possibility is adding support for multiple targets or mobile targets, and to accommodate more realistic signal



(a)



(b)

Fig. 8: The false positive and false negative error rate for three different range thresholds.

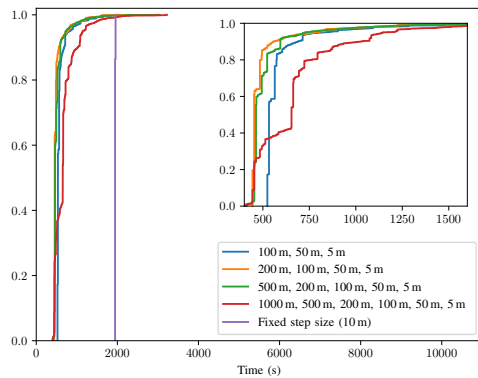
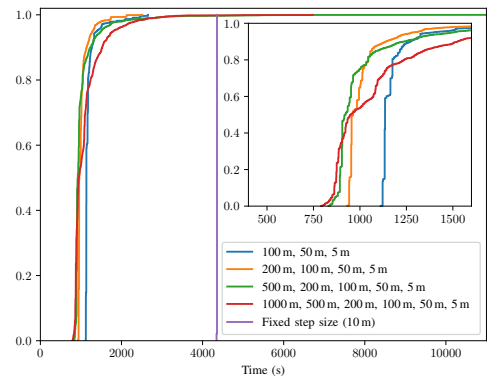
(a) $R = 1628$ m(b) $R = 3628$ m

Fig. 9: The ECDF of time taken to reach within 10 m of the transmitter for four sets of threshold distances.

propagation and detection models. One final avenue is a real implementation of the system to verify our model and results.

REFERENCES

- [1] S. Mayer, L. Lischke, and P. W. Wozniak, "Drones for Search and Rescue," in *Proc. First International Workshop on Human-Drone Interaction, Ecole Nationale de l'Aviation Civile [ENAC]*, Glasgow, United Kingdom, May 2019.
- [2] P. Doherty and P. Rudol, "A UAV Search and Rescue Scenario with Human Body Detection and Geolocation," in *Proc. 20th Australasian Joint Conference on Artificial Intelligence (AI 2007)*, Gold Coast, Australia, Dec. 2007.
- [3] M. Silvagni, A. Tonoli, E. Zenerino, and M. Chiaberge, "Multipurpose UAV for Search and Rescue Operations in Mountain Avalanche Events," *Geomatics, Natural Hazards and Risk*, vol. 8, no. 1, pp. 1–16, 2016.
- [4] D. Erdos, A. Erdos, and S. E. Watkins, "An Experimental UAV System for Search and Rescue Challenge," *IEEE Aerospace and Electronic Systems Magazine*, vol. 28, no. 5, pp. 32–37, May 2013.
- [5] P. Pace, G. Aloï, G. Caliciuri, and G. Fortino, "A mission-oriented coordination framework for teams of mobile aerial and terrestrial smart objects," *Mobile networks and applications*, vol. 21, no. 4, 2016.
- [6] D. Barry, A. Willig, and G. Woodward, "An Information-Motivated Exploration Agent to Locate Stationary Persons with Wireless Transmitters in Unknown Environments," *MDPI Sensors*, 2021.
- [7] G. Duchêne and F. Quitin, "Detecting the source of an RF signal with a transceiver-equipped UAV," in *14th International Symposium on Wireless Communication Systems*, 2017.
- [8] S. Venkateswaran *et al.*, "RF source-seeking by a micro aerial vehicle using rotation-based angle of arrival estimates," in *2013 American Control Conference*, 2013.
- [9] M. Petitjean, S. Mezhoud, and F. Quitin, "Fast localization of ground-based mobile terminals with a transceiver-equipped UAV," in *2018 IEEE 29th Annual International Symposium on Personal, Indoor and Mobile Radio Communications (PIMRC)*, 2018, pp. 323–327.
- [10] M. A. A. Careem, J. Gomez, D. Saha, and A. Dutta, "RFEye in the sky," *IEEE Transactions on Mobile Computing*, 2020.
- [11] Z. Chen, S. Yeh, J.-F. Chamberland, and G. H. Huff, "A sensor-driven analysis of distributed direction finding systems based on UAV swarms," *Sensors*, vol. 19, no. 12, 2019.
- [12] J. Werner *et al.*, "Sectorized antenna-based DoA estimation and localization: Advanced algorithms and measurements," *IEEE Journal on Selected Areas in Communications*, vol. 33, no. 11, 2015.
- [13] F. Gunnarsson *et al.*, "Downtilted base station antennas - a simulation model proposal and impact on HSPA and LTE performance," in *2008 IEEE 68th Vehicular Technology Conference*, 2008, pp. 1–5.
- [14] 3GPP, "Physical layer aspect for evolved universal terrestrial radio access (UTRA)," 3GPP, Tech. Rep. TR25.814 v7.1, October 2006.
- [15] A. Hakkarainen *et al.*, "Reconfigurable antenna based doa estimation and localization in cognitive radios: Low complexity algorithms and practical measurements," in *9th International Conference on Cognitive Radio Oriented Wireless Networks*, 2014, pp. 454–459.
- [16] N. I. Fisher and T. Lewis, "Estimating the common mean direction of several circular or spherical distributions with differing dispersions," *Biometrika*, vol. 70, no. 2, pp. 333–341, 1983.
- [17] R. Stansfield, "Statistical theory of d.f. fixing," *Journal of the Institution of Electrical Engineers - Part IIIA: Radiocommunication*, vol. 94, pp. 762–770(8), December 1947.
- [18] S. S. Haykin, *Communication Systems*, 4th ed. New York: Wiley, 2001.